

Buoyancy Effects in Turbulent Mixing: Sampling Turbulence in the Stratified Ocean

Carl H. Gibson*

University of California, San Diego, La Jolla, Calif.

Stable stratification in the ocean and atmosphere tends to suppress turbulence, mixing, and vertical diffusion. Active turbulence is often confined to isolated patches which occur intermittently in time, decay rapidly, and occupy a small volume fraction of most layers. Estimates of mean dissipation rates ϵ and χ of turbulent velocity and temperature from short vertical or short horizontal records in a layer may underestimate the space-time mean values by orders of magnitude under common oceanic conditions due to undersampling errors. If χ is log-normal the short record sample values will probably be less than the space average for the layer by a factor of $\exp(3\sigma^2/2)$, the ratio of mean/mode for a log-normal distribution, where σ^2 is the variance of $\ln\chi$. Variation of ϵ and χ with depth from dropsondes actually may be a better indication of the vertical variation of $\sigma_{\ln(\epsilon, \chi)}^2$ than variation of $(\epsilon, \chi)_{\text{mean}}$; for example, dropsonde values of ϵ and χ in the strongly stratified core region of equatorial undercurrents (probably large σ) are much smaller than in the sheared layers above and below (probably smaller σ). Towed body ϵ and χ values in the core are larger than either the dropsonde core or shear-layer values, possibly because tow bodies collect more data and include more of the active patches which dominate the average for a layer. Space averages may underestimate space-time averages if the space average turbulence is intermittent in time. A tentative correction procedure is described based on information about previous active turbulence preserved by fossil turbulence microstructure. Most oceanic temperature microstructure appears to be fossil turbulence, suggesting such a correction procedure may permit inferences about the turbulence processes occurring a few hours or even days prior to the actual microstructure measurements.

I. Introduction

THE purpose of the present paper is to describe some effects of stable stratification on turbulence and turbulent mixing, particularly in the ocean and atmosphere, and to discuss some resulting problems in sampling turbulence in the ocean. Fluids in nature typically form stratified layers in a gravity field. Buoyancy forces develop which prevent and suppress turbulence. Consequently, even though a complex field of internal waves and shears may exist in a stratified fluid, turbulence may be confined to scattered intermittent patches. Vertical diffusion and mixing may be inhibited strongly. Measurement techniques must take into account the patchiness and intermittency of stratified turbulence to be reliable.

Vertical diffusion in the atmosphere, oceans, and lakes by nonturbulent molecular processes is very slow. Though the turbulence may be constrained by buoyancy to a small volume fraction of space time it may still be the dominant diffusion process. Smog accumulation over cities and eutrophication of lakes and seas are examples of the adverse effects of turbulence inhibited by buoyancy. Smoke stacks and oceanic sewer outfalls take advantage of the weak diffusivity of stratified flows to prevent diffusion of smoke to the ground or sewage to the sea surface by discharging into stratified layers.

Theoretical and experimental studies of stratified turbulence and turbulent mixing are in an early stage of development, as discussed in Turner's book¹ on the subject. Radar and sonar backscatter observations show a patchy

layered pattern of presumably turbulent² refractive index fluctuations related to internal wave motions in the stratified atmosphere and ocean, respectively, but few direct measurements of the local velocity and density structure have been available for detailed analysis. Laboratory measurements have been useful, but have uncertain applicability to natural conditions because of the comparatively limited range of length and time scales.

Atmospheric turbulence studies generally have been in the surface boundary layer within neutrally or unstably stratified flows. Aircraft studies have shown the existence of "clear air turbulence" patches in the stratified layers, but because of the high speed of the platform and limited response of the sensors little has been done to document less active regions.

Studies of small-scale velocity and temperature fluctuations in the ocean have been carried out for nearly twenty years from towed bodies and submarines.³ However, oceanic turbulence and mixing signals are extremely weak compared to those produced by laboratory and atmospheric flows. Frequency response and spatial resolution requirements are high. Consequently, most towed body and submersible measurements of oceanic turbulence have been contaminated to some extent by platform noise. Advances in instrumentation and techniques to decouple the towed body from ship motions have improved signal to noise ratios. Some recent results will be discussed in later sections of this paper.

To avoid platform noise, several vertically profiling instruments have been developed either with internal recording⁴ for free-falling devices or with thin wires for data transmission and instrument retrieval.⁵ These vertical profilers, or "dropsondes," have been deployed in a wide variety of oceanic regions to depths of a few kilometers. Signal to noise ratios are excellent below surface wave depths, and because such instruments descend slowly, 10-50 cm/s, frequency response requirements are not severe. Unfortunately, a single vertical cut may not provide enough data to characterize the turbulence and mixing processes of a stably stratified oceanic layer because of the patchiness and intermittency of the processes.

Presented as Paper 80-1334 at the AIAA 13th Fluid and Plasma Dynamics Conference, Snowmass, Colo., July 14-16, 1980; submitted Sept. 16, 1980; revision received April 21, 1981. Copyright © American Institute of Aeronautics and Astronautics, Inc., 1980. All rights reserved.

*Professor of Engineering Physics and Oceanography; Departments of Applied Mechanics and Engineering Sciences and Scripps Institution of Oceanography.

Temperature fluctuations are generally easier to measure than velocity fluctuations from either towed bodies or dropsondes. Consequently, most reported oceanic microstructure signals are temperature. Schedvin⁶ has examined temperature signals from various stratified regions below a wind mixed layer using a profiling towed body. The microstructure was found to be quite inhomogeneous in the horizontal direction, with variation of the thermal dissipation rate by several orders of magnitude. Spectra at different angles of attack taken from statistically homogeneous regions showed that most of the microstructure was vertically stratified at the largest scales and approached isotropy only at small scales, suggesting that the turbulence that generated the microstructure had been damped out or strongly affected by buoyancy. Such temperature microstructure remnants of previous active turbulence in nonturbulent fluid are termed "fossil temperature turbulence."² Properties of fossil temperature, salinity, and vorticity turbulence have been discussed by Gibson.⁷ Using a turbulence activity parameter A_T (Sec. IV) criterion it was found that the towed body temperature microstructure measurements of Schedvin⁶ and all of the published temperature microstructure data from dropsondes indicates a state of complete or partial fossilization. Thus it appears that neither the towed body nor dropsonde records have been of adequate length or time duration to observe the rare turbulence events that produce the observed microstructure.

For nonstratified flows such as the atmospheric boundary layer near the surface, it has been possible to develop and test equations relating the viscous and thermal dissipation rates to the mean momentum and heat fluxes. Similar "dissipation flux" relations have been proposed for stratified media by Osborn and Cox.⁸ However, measurement of average dissipation rates are complicated by buoyancy effects such as fossilization and the intermittency in time and patchiness in space of the turbulence. In the following sections, the magnitudes and possible means of accounting for such buoyancy effects will be discussed.

II. Dissipation Flux Estimates

In steady, homogeneous, nonstratified turbulent shear flows the production of turbulent kinetic energy and scalar variance are balanced by the viscous and diffusive dissipation rates ϵ and χ , respectively, where

$$\epsilon = 2\nu e_{ij}^2; \quad e_{ij} = \frac{1}{2} \left(\frac{\partial u_i}{\partial x_j} + \frac{\partial u_j}{\partial x_i} \right); \quad i, j = 1, 2, 3$$

$$\chi = 2D \left(\frac{\partial \theta}{\partial x_i} \right)^2$$

and D, ν are molecular diffusivities of θ and momentum.

The production rate of turbulent kinetic energy per unit mass is $-\overline{u'_1 u'_3} (\partial \overline{u}_1 / \partial x_3)$ and the production rate of θ variance is $-2\overline{u'_3 \theta} (\partial \overline{\theta} / \partial x_3)$, where the turbulent momentum and θ fluxes and gravity are in the x_3 direction, and the mean flow is in the x_1 direction. Primes indicate fluctuations about mean values and overbars indicate averages (see Tennekes and Lumley⁹ for details, pp. 63 and 65).

Since the mean shear and mean scalar gradients are usually easy to measure, estimates of the fluxes can be made from measurements of ϵ and χ . Comparisons of such dissipation fluxes $\epsilon / (\partial \overline{u}_1 / \partial x_3)$ and $\chi / 2(\partial \overline{\theta} / \partial x_3)$ with direct measurements of $-\overline{u'_1 u'_3}$ and $-\overline{u'_3 \theta}$ in careful atmospheric boundary-layer experiments have been quite successful.¹⁰

Osborn and Cox⁸ have proposed that $-\overline{\theta u'_3}$ may equal $\chi / 2(\partial \overline{\theta} / \partial x_3)$ in the ocean. Osborn¹¹ has estimated temperature fluxes in the Atlantic Equatorial Undercurrent and other ocean regions from χ and $\partial \overline{\theta} / \partial x_3$ measurements from dropsondes.¹²

By assuming that the flux Richardson number $R_f = \overline{PE} / \epsilon$ is constant and that $-(\overline{PE} + \epsilon)$ equals the turbulent kinetic energy production rate \overline{KE} , Osborn¹¹ also estimated vertical density flux rates, where $\overline{PE} = g \overline{u'_3 \rho'} / \rho$ is the potential energy production rate per unit mass due to turbulent mixing, g the acceleration of gravity, and ρ the density.

Gregg^{13,14} has used dropsonde χ measurements to estimate eddy diffusivity coefficients K_T for temperature in a wide variety of ocean regions, where $K_T = \chi / 2(\partial \overline{T} / \partial x_3)^2$. Generally such dissipation eddy diffusivities from dropsonde dissipation rate measurements are much smaller than bulk K_T estimates from mean temperature, salinity, or oxygen content measurements. In a steady flow with current v_x the bulk vertical eddy diffusivity is often estimated as $v_x (\partial s / \partial x) / (\partial^2 s / \partial z^2)$, where s is a conserved scalar fluid property. Sverdrup et al.¹⁵ state (p. 483) that most bulk

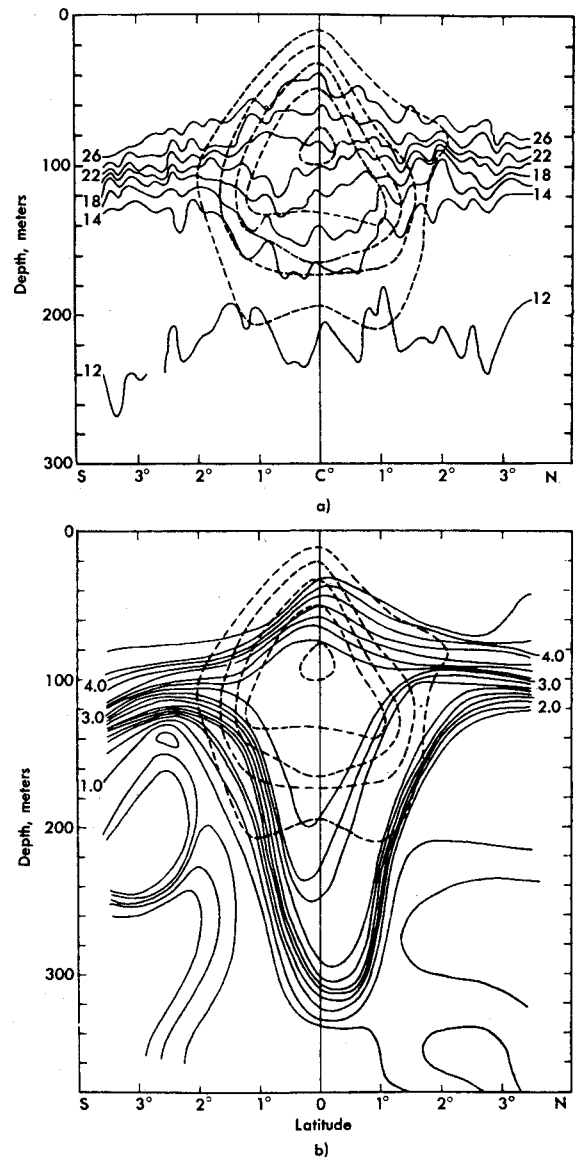


Fig. 1 Velocity cross section (dashed lines) superimposed on a) temperature and b) oxygen sections through the Cromwell Current at longitude 140°W.³⁰ The broadening of isotherms and iso-oxygen surfaces near the core of the undercurrent at 100 m on the equator suggests strong turbulent mixing. Towed bodies at the core give $\epsilon \approx 0.1 \text{ cm}^2/\text{s}^3$ and $\chi \approx 10^{-4} \text{ C}^2/\text{s}$ (strong turbulence and turbulent mixing) but dropsondes give $\epsilon \sim 10^{-5} \text{ cm}^2/\text{s}^3$ and $\chi \sim 10^{-8} \text{ C}^2/\text{s}$ (laminar flow and mixing only by molecular diffusion). The discrepancy may be due to large sampling errors in the dropsonde estimates, which are based on short records of the extremely patchy and intermittent turbulence process.

Table 1 Hydrodynamic states in Atlantic Equatorial Undercurrent implied by dropsonde ϵ measurements of Osborn¹¹

Layer	ϵ , cm^2/s^3	N , rad/s	L_R , cm	L_K , cm	$L_R/10L_K$	Hydrodynamic state (implied)
High shear above core, 20-60 m	3×10^{-3}	1.5×10^{-2}	30	0.15	20	Weakly turbulent
Core region, 60-110 m	3×10^{-5}	2.4×10^{-2}	1.5	0.49	0.31	Laminar
High shear below core, 110-148 m	5×10^{-4}	1.0×10^{-2}	22	0.24	9.1	Weakly turbulent

oceanic K_T values are in the range 3-90 cm^2/s . However, Gregg reports K_T values in the North Pacific Gyre of only 0.1 cm^2/s . Osborn¹¹ reports even smaller K_T values in the core (layer of maximum speed) of the Atlantic Equatorial Undercurrent, ranging from 0.006 to 0.04 cm^2/s compared to a value of 25 cm^2/s estimated by Williams and Gibson¹⁶ in the core of the Pacific Equatorial Undercurrent from measurements using a towed body. Measurement discrepancies of 3-4 orders of magnitude are remarkable, even in the sometimes uncertain field of experimental turbulence, and require explanation.

Figure 1 shows the distribution of temperature, oxygen, and velocity as a function of depth in a north south section of the Pacific Equatorial Undercurrent, or Cromwell Current, measured by Knauss and discussed by von Arx¹⁷ (p. 176). A huge volume of water, comparable to the Gulf Stream, flows from west to east beneath east to west surface currents, with maximum relative velocity of about 3 knots at a depth of about 100 m. The Atlantic Equatorial Undercurrent is similar in size, speed, direction, and depth. The cause of these currents is unknown.

A very striking feature of the temperature distribution at the equator is the broadening of the thermocline about the undercurrent. The undercurrent is shown by dashed lines of constant speed. Similarly the oxygen concentration spreads about the current, with concentrations found at 150-m depth 2-deg north and south of the equator penetrating over 300-m depth at 0-deg latitude. According to Osborn,¹¹ K_T and $K\rho$ values in the high shear layers above the core of the undercurrent are in the range 1-4 cm^2/s , but in the 20-40-m thick core region they fall to only 0.006-0.04 cm^2/s . In the sheared zone below the core they abruptly rise to the range 0.2-3 cm^2/s . This pattern of K_T values seems inconsistent with the observed oxygen and temperature distributions. If heat and oxygen are diffusing down through the current, such large gradients in diffusivity should be accompanied by large gradients in the diffused quantities, yet no such strong gradients in either temperature or oxygen appear in the distributions shown in Fig. 1. Either a system of lateral advection or sources and sinks must be postulated, or else the eddy diffusivities estimated from the dropsonde dissipation rates must not be representative of the actual average values for the layers.

Since a dropsonde makes only a single vertical cut through each stratified layer, it is necessary to consider the possibility that the average dissipation rate for the sample is not representative of the average value of dissipation rate in the layer. This is a familiar problem in atmospheric boundary-layer turbulence dissipation measurements, where it is usually necessary to average several kilometers of air to obtain convergence of ϵ and χ averages. ϵ and χ are quite intermittent because of the high Reynolds number of the atmospheric flow.

The thickness of statistically independent stratified layers should be the maximum scale of vertical turbulence $L_R \equiv (\epsilon/N^3)^{1/2}$, or Ozmidov length, where N is the buoyancy frequency $[(g/\bar{\rho})(\partial\bar{\rho}/\partial z)]^{1/2}$. Osborn's ϵ values from the undercurrent core are about $3 \times 10^{-5} \text{cm}^2/\text{s}^3$ with N values of

about $2.4 \times 10^{-2} \text{rad/s}$, so Ozmidov lengths are only about 1.4 cm. Even in the sheared layers above the core where $\epsilon = 3 \times 10^{-3} \text{cm}^2/\text{s}^3$, $K\rho = 4 \text{cm}^2/\text{s}$, and $N = 1.5 \times 10^{-2} \text{rad/s}$, L_R values are only 30 cm. Below the core, where $\epsilon \sim 5 \times 10^{-4} \text{cm}^2/\text{s}^3$, $N = 10^{-2} \text{rad/s}$ and $K\rho \sim 1 \text{cm}^2/\text{s}$, L_R is only 23 cm.

In order for the turbulence to exist,^{7,28} L_R must be larger than the viscous scale $\approx 10L_K = 10(\nu^3/\epsilon)^{1/4}$. This conclusion follows from $(L_R)_t \sim (L_K)_t$, $R_i = N^2/(\partial u/\partial z)^2 = 1/4$, and $(\partial u/\partial z)^2 \approx 2\epsilon_t/15\nu$ at the transition to turbulence in a stratified fluid, which gives $\epsilon_t = 30\nu N^2$. Recent measurements in a stratified turbulent grid flow in a water tunnel by Stillinger and Helland²⁹ give $\epsilon_t = 23\nu N^2$. However, $10L_K$ is 9 cm in the core and 1.5 and 2.4 cm in the shear layer above and below the core, respectively. Therefore, using the dropsonde measurements of ϵ as estimates of the average for these regions, the undercurrent core region should be completely nonturbulent and the sheared layers only weakly turbulent. Table 1 summarizes the parameters and implied hydrodynamic states for the three regions of the Atlantic Equatorial Undercurrent discussed by Osborn.¹¹

Diffusion of oxygen by molecular processes through a 20-m thick nonturbulent layer is astronomically slow. The diffusion time constant L^2/D for such a layer is of order 1000 yr. Extraordinarily high levels of organic productivity characteristic of equatorial regions requires rapid vertical exchange of oxygen and nutrients. It has usually been assumed that the high equatorial productivity is a result of strong turbulent mixing produced by the undercurrent, contrary to the dropsonde evidence that the core of the current is nonturbulent and the shear layers only weakly turbulent.

If a stratified layer is not horizontally homogeneous a single vertical sample $\bar{\epsilon}(L_R, z)$ will probably not equal the actual average $\bar{\epsilon}(L \rightarrow \infty, z)$, where L is the length scale of the averaging volume. If the layer is quite patchy, the random variable $\bar{\epsilon}(L_R, z)$ may have a wide probability density function with mode very much smaller than the mean. If the dissipation rates in all layers of the core region were identically distributed, then a vertical profile might be considered a collection of a large number of independent samples of the very thin, weakly diffusive layers in the 20-40-m thick core, so the vertical averages of these samples might be representative of the horizontal average of each layer. However, if the actual average values are large and variable, and if the patchiness varies with depth, the vertical average is of little value: the average of nonrepresentative samples does not become representative.

Measurements of ϵ in the core of the Atlantic Equatorial Undercurrent by Belyaev et al.^{18,19} using a towed body indicate extreme patchiness and mean values much larger than the dropsonde values. Local values greater than 1 cm^2/s^3 are reported with mean values of 0.1 cm^2/s^3 . ϵ and χ values from other areas were generally much larger than those inferred from dropsondes.

Similarly, χ values measured by Williams and Gibson¹⁶ from a towed body in the core regions of the Pacific Equatorial Undercurrent are much larger than dropsonde values. Gregg¹³ reports χ values of $10^{-8} \text{C}^2/\text{s}$ compared to $10^{-4} \text{C}^2/\text{s}$ for the tow-body measurements from the same

depth range. The Osborn and Bilodeau¹² values of χ from the core of the Atlantic Equatorial Undercurrent overlap Gregg's with χ in the range 10^{-8} - 10^{-6} °C²/s. As Gregg¹³ points out, the towed-body measurements are much noisier than those from dropsondes, which might account for the fact that towed-body estimates of ϵ and χ are consistently larger. However, Gregg's suggestion¹³ that the towed-body temperature signal could be vertical vibrations of the sensors in a vertical temperature gradient was shown to be unlikely by Schedvin.⁶ Schedvin used accelerometers to measure vibrations of the same towed body used by Williams and Gibson¹⁶ in a comparable vertical temperature gradient, and found that this sort of vibrational temperature gradient noise was 10^{-7} less than the measured signal (pp. 134 and 135)⁶ at the dissipation scales. Another possibility is that the dropsondes may undersample ϵ and χ when the turbulence is very patchy and these quantities range over 6 orders of magnitude. Gregg¹³ observed well-mixed patches in the core region of the Pacific Equatorial Undercurrent of vertical thickness about 2 m. If these patches were caused by turbulence, the originally active turbulence ϵ_0 values should be about $1.7 \text{ cm}^2/\text{s}^3$, close to the extreme Belyaev et al.^{18,19} values, and original χ_0 values should be about $1.1 \times 10^{-3} \text{ °C}^2/\text{s}$ (see Sec. IV).

If the turbulence is intermittent as well as patchy, even a very large number of samples in a layer from either a tow body or dropsonde may underestimate the averages unless they are carried out over a long time period. In Sec. IV the possibility of using fossil turbulence properties to compensate for intermittency in time is discussed.

III. Probability Laws for Dissipation Rates

Average ϵ and χ values are important parameters of any flow or mixing process. As indicated in the last section, the variability in time and space of ϵ and χ may affect the sampling procedures required to estimate true mean values. Furthermore, the probability laws describing the variability of ϵ and χ are determined by the physical processes and may provide important information about these processes. It is as important to know whether ϵ and χ are homogeneous and stationary or patchy and intermittent as it is to know their averages. If ϵ and χ are patchy and intermittent, it is important to determine the "distances between patches" and the "times between bursts" (to use a bimodal description of the probability laws).

Dissipation rates in high Reynolds number nonstratified flows become increasingly intermittent and patchy as the Reynolds number increases. Kolmogoroff²⁰ proposed a refinement to his earlier universal similarity hypotheses to take this into account, assuming that the logarithm of ϵ should be normally distributed with variance increasing with Reynolds number. Both ϵ and χ have been shown to have log-normal tendencies in high Reynolds number nonstratified flows.²¹

In stratified flows the physical arguments in support of log normality for ϵ and χ are complicated by the existence of several mechanisms besides the turbulence cascade that can produce dissipation. Some of these are breaking internal waves, double diffusive instabilities, and sources of random forcing such as surface winds. Satellite photographs of sea surface temperature and atmospheric cloud patterns show that a form of two-dimensional turbulence exists in the atmosphere and ocean. This suggests a cascade of temperature variance from large to small scales due to two-dimensional turbulent mixing. Possibly the final stage of mixing occurs in regions of strong horizontal mean temperature gradients, or fronts, where three-dimensional turbulence formation is enhanced. If the alternate sources of dissipation, particularly internal wave breaking, also concentrate at the fronts, then stratified dissipation may approach log normality.

If each scale of two-dimensional turbulent mixing is independent of each larger and smaller scale of the cascade, the

random variable

$$X(r) = \chi(r) / \chi(2r), \quad L > r > L_K \quad (1)$$

should be statistically independent of $X(r' > 2r)$ and $X(r' < r/2)$, where $\chi(r)$ is the average over a horizontal scale r , L the largest scale of the two-dimensional turbulence, L_K the viscous scale $(\nu^3/\epsilon)^{1/4}$, and $L > r' > L_K$. If $L \gg L_K$ then we may compose the identity

$$\begin{aligned} \chi(r) &= \frac{\chi(r)}{\chi(2r)} \frac{\chi(2r)}{\chi(4r)} \cdots \frac{\chi(kr)}{\chi(L)} \chi(L) \\ &= X(r) X(2r) \cdots X(kr) \chi(L) \end{aligned} \quad (2)$$

Taking the logarithm of Eq. (2) gives

$$\ln \chi(r) = \ln X(r) + \ln X(2r) + \cdots + \ln X(kr) + \ln \chi(L) \quad (3)$$

Since from Eq. (3) the random variable in $\chi(r)$ is the sum of many independent random variables $\ln X$, then according to the central limit theorem, $\ln \chi(r)$ should be normally distributed. The expected value in $\ln \chi(r)$ is the sum of expected values of the other random variables in Eq. (3), but $E(\ln X) = 0$ so $E[\ln \chi(r)] = E[\ln \chi(L)]$. The variance of $\ln \chi(r)$ is the sum of the variances of the $\ln X$ variables. If the $\ln X$ variables all have variance $\sigma_{\ln X}^2$ then $\ln \chi(r)$ should have variance $k\sigma_{\ln X}^2$, where $k = \log_2(L/L_K)$.

Log-normal random variables are generally very intermittent, with mode values near zero and much less than the mean or median values. As an example, suppose at some depth in the ocean horizontal temperature regions of scale 100 km (the width of the Cromwell Current is 200 km, and has large meanders) are mixed by two-dimensional turbulence down to a diffusive scale of about 10 cm. Then, $L/L_K = 10^6$, $\log_2 10^6 = k = 20$, and from Eq. (3) $\ln \chi(10 \text{ cm})$ will be Gaussian with mean μ and variance $\sigma^2 = 20\sigma_{\ln X}^2$. The mode of a log-normal random variable is $\exp(\mu - \sigma^2)$ and the mean is $\exp(\mu + \sigma/2)$, so the ratio mean/mode = $\exp[(3/2)\sigma^2]$. Assuming (rather arbitrarily, to compare with the data of Figs. 2-4) $\sigma_{\ln X}^2 = 0.2$ gives $\sigma^2 = 4$ for our example with mean $\exp 6 = 403$ times larger than the mode. The median of χ is $\exp \mu$, so the (mean/median) ratio is $\exp \sigma^2/2 = 7.38$. Therefore half of the ϵ samples will be at least a factor of 7 less than the mean $E(\chi)$. The probability density function of χ is $(1/\chi\sqrt{2\pi\sigma}) \exp[-(\ln \chi - \mu)^2/2\sigma^2]$ so the probability density of the mean is $\exp(-9\sigma^2/8) \approx 1/90$ times that of the mode.

In attempting to estimate the mean χ at any depth it is important to know whether χ is patchy, and whether the patchiness varies with depth. Thus, if χ is log normal and μ and σ do not vary with depth, a single vertical profile can be used as a large number of representative samples of χ if the layer thickness is small compared to the profile depth. However, μ and σ generally will vary considerably with depth, since each layer depends on different sources of variance with different time and space scales. For example, μ and σ for the shear layers above and below the core of the equatorial undercurrent are probably quite different from each other and from μ and σ for the core. Thus if σ varies with depth, the ratio of (mean/mode) = $\exp(3\sigma^2/2)$ will vary with depth. The observation that the sample values of χ and ϵ in the core region are less than sample values in the sheared layers may only indicate that $\sigma_{\text{core}} > \sigma_{\text{shear}}$, rather than that $(\chi, \epsilon)_{\text{core}} < (\chi, \epsilon)_{\text{sheared}}$. In fact, if σ is large in all layers, then it is possible that $(\chi, \epsilon)_{\text{dropsonde}} < (\chi, \epsilon)_{\text{mean}}$ simply because $(\chi, \epsilon)_{\text{dropsonde}} \approx (\chi, \epsilon)_{\text{mode}} < (\chi, \epsilon)_{\text{mean}}$ when σ is large. This may provide an explanation for the fact that dropsonde estimates of vertical diffusivities from dissipation measurements have been much less than those estimated from mean quantities in the same regions.

Horizontal profiling of dissipation rates have provided little information about μ and σ because noise levels have been higher than $(\chi, \epsilon)_{\text{mode}} \cdot \chi_{\text{mode}} < 10^{-8} \text{ °C}^2/\text{s}$ and $\epsilon_{\text{mode}} < 10^{-5} \text{ cm}^2/\text{s}^3$ in most ocean regions, judging from the dropsonde

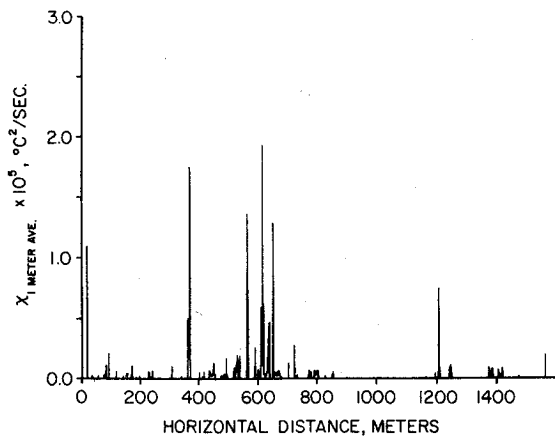


Fig. 2 Temperature dissipation rate χ measured from a towed body in the layer of maximum stratification ($0.3^\circ\text{C}/\text{m}$) at 36-m depth (Sept. 7, 1977, 50°N 145°W , MILE mixed-layer experiment). The most probable value (mode) of χ is less than $10^{-7}^\circ\text{C}^2/\text{s}$. A few active microstructure patches dominate the mean value $\bar{\chi} = 0.7 \times 10^{-6}^\circ\text{C}^2/\text{s}$. The patches are all fossil temperature turbulence, with A_T values less than 1.0, shown as triangles in Fig. 5.

measurements, compared to about ($10^{-7}^\circ\text{C}^2/\text{s}$, $10^{-3} \text{cm}^2/\text{s}^3$) towed body (χ, ϵ) noise levels. To estimate the probability density function of a random variable from a histogram, the noise must be less than the mode or the peak of the pdf will not be resolved. Another difficulty is that the extremely large values of χ and ϵ in the dominant patches may require frequency response, dynamic range, and spatial resolution beyond the capabilities of the sensors and electronics, so even if such patches are encountered, their contributions may be attenuated.

Figure 2 shows a recent horizontal profile of χ estimated from a microconductivity probe on a towed body in the thermocline taken during the 1977 MILE mixed-layer experiment at ocean station P (50°N , 145°W).²⁵ Simultaneous microbead thermistor signals show that the conductivity signal is dominated by temperature at frequencies up to 25 Hz, and the shape of the diffusive roll-off of the microconductivity signal spectrum suggests that the salinity contribution to conductivity gradients is negligible from frequencies less than 200 Hz. The conductivity probe was mounted on a streamlined body with a large wing and a tether-pulley arrangement to resist vertical motions and also reduce vibrational forces transmitted from the tow cable to the tow body. Vertical excursions of the towed body about the mean depth of 36 m were usually only 10-30 cm at the surface wave period with maximum deviation of less than a meter over several kilometers.

χ values were calculated from spectra computed for 1-m records, over a spatial frequency bandwidth of 2-130 cpm. As shown in Fig. 2, the 1-m averaged χ values vary over a wide range, from a noise level of about $10^{-7}^\circ\text{C}^2/\text{s}$ to peak values over $10^{-5}^\circ\text{C}^2/\text{s}$. $\bar{\chi}$ for the total record is about $10^{-6}^\circ\text{C}^2/\text{s}$. Most of $\bar{\chi}$ is due to a small fraction of the total record. The most active 1-m records are not randomly distributed, but tend to cluster together. Most of the 1-m records with χ less than $\bar{\chi}$ are dominated by noise, which means they have χ less than $10^{-7}^\circ\text{C}^2/\text{s}$.

Figure 3 shows a comparison of χ with log normality for the data of Fig. 2. Average χ values for 1-m data records were computed with and without correction for noise. The noise correction was accomplished by subtracting the spectrum from quieter regions from the record spectrum and setting high wavenumber variance to zero above the first point of spectral overlap. Two noise corrected probability distributions are shown corresponding to spectra from two different quieter regions. By this criterion χ for about half of the data records was set to zero for one of the correction spectra, as shown by the horizontal portion of the upper

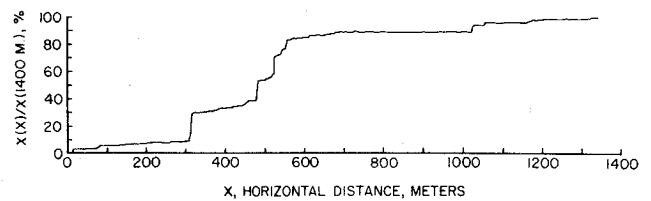


Fig. 3 Log-normality test of χ averaged over 1-m records, with and without noise correction. Same data as Fig. 2.

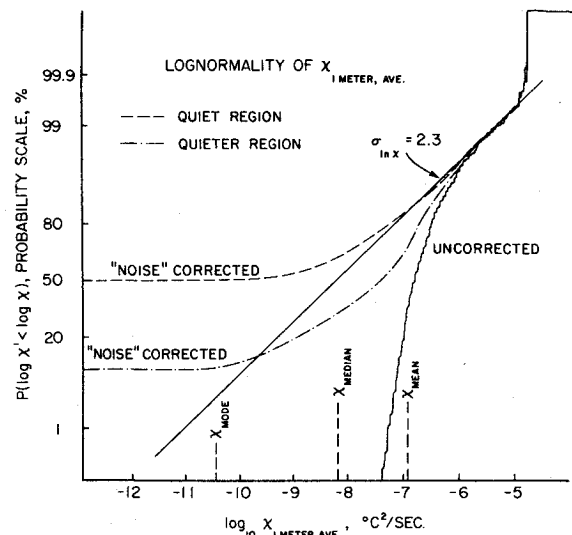


Fig. 4 Accumulated percent temperature gradient variance, expressed as $\chi(X)/\chi(1400 \text{ m})$, vs horizontal distance X . Same data as Figs. 2 and 3.

"noise corrected" probability curve in Fig. 3. The lower noise corrected probability curve is an upper bound for the true probability and the uncorrected curve is a lower bound. For the range 10^{-5} - $10^{-6}^\circ\text{C}^2/\text{s}$ the χ curves converge to a straight line corresponding to a log-normal distribution with standard deviation $\sigma_{\ln \chi} = 2.3$ and $\chi_{\text{median}} \approx 10^{-8}^\circ\text{C}^2/\text{s}$. The deviation from log normality at large χ values can be attributed to the small number of samples with extremely large χ . The drooping form of the uncorrected probability curve is partly due to noise but may also have a physical basis, reflecting the minimum value $\chi_{\text{min}} = 2D(\partial T/\partial Z)^2$ imposed by the ambient mean vertical temperature gradient, which can never be zero. χ_{min} for the data is about $10^{-8}^\circ\text{C}^2/\text{s}$. The drooping form also seems to appear in the lower corrected curve and in other computed probability curves not reported here.

It is clear from Figs. 2 and 3 that χ is very patchy in the 36-m depth layer, located below the mixing layer in the strongest temperature gradient portion of the seasonal thermocline. Most of the temperature gradient variance of the record is contained in a few isolated patches. Figure 4 shows accumulated variance as a function of horizontal distance for the data of Fig. 2. Increases occur in sharp steps corresponding to the patches. Eight patches, each with length 5-10 m and $\chi = 10^{-4}$ - $10^{-6}^\circ\text{C}^2/\text{s}$, give over 80% of the record mean; the rest of the record is close to or below the instrument noise level. A small data sample from either a towed body or dropsonde at this depth will tend to underestimate the space average χ by a large factor, of order 10. At least 100 m of record must be averaged for $\bar{\chi}$ to converge within a factor of 2.

Whether the 1.4 km record shown in Fig. 2 will be adequate to determine the space average χ (at 36-m depth) for the 25-km MILE array (or whether the MILE array adequately characterizes the North Pacific Gyre) has not been determined.

correction for spatial patchiness in many ocean regions, and dropsonde measurements will require corrections almost everywhere. The discrepancy between diffusion coefficients in the ocean estimated from dropsonde measurements of dissipation rates and the much larger diffusion coefficients estimated from either mean properties or towed-body dissipation rates may be explained as the result of undersampling of the patchy dissipation by the dropsondes.

Even less is known of the effects of time intermittency on estimates of space-time averages in stratified turbulence, except that intermittency exists and also probably will cause short time averages over space to underestimate the actual space-time average. An attempt was made to show how parameters of fossil turbulence might be used to convert instantaneous values of C to the time average over the life of the fossil patch.

In summary, it appears that oceanic measurements of local dissipation rates by vertical profilers (dropsondes) probably underestimate the space-time average of most layers by about 2-4 orders of magnitude. Corrections for patchiness and intermittency such as those described in this paper would seem to be mandatory if this sampling technique is used. However, the probability laws of stratified turbulence and the decay rates of fossil turbulence which are required in such correction schemes are poorly understood at this time. Horizontal profiling in each layer will give a much larger sample size, but the data processing requirements are enormous. The optimum sampling technique may require a combination of horizontal and vertical profiling plus a much better knowledge of the probability laws and fluid mechanics of stratified turbulence.

Acknowledgments

Support for this work was provided by NSF ENG 27398. The data for Figs. 2-4 were collected by John Schedvin and the analysis and plotting was done by Libe Washburn.

References

- ¹Turner, J. S., *Buoyancy Effects in Fluids*, Cambridge University Press, 1973, pp. 91-164.
- ²Hogstrom, V., Misme, P., Ottersten, H., and Phillips, O. M., "Report of Working Group: Fossil Turbulence," edited by J. D. Woods, *Radio Science*, Vol. 4, Dec. 1969, pp. 1365-1367.
- ³Grant, H. L., Moilliet, A., and Vogel, W. M., "Some Observations of the Occurrence of Turbulence in and Above the Thermocline," *Journal of Fluid Mechanics*, Vol. 34, Dec. 1968, pp. 443-448.
- ⁴Gregg, M. C., Cox, C. S., and Hacker, P. W., "Vertical Microstructure Measurements in the Central North Pacific," *Journal of Physical Oceanography*, Vol. 3, Oct. 1973, pp. 458-469.
- ⁵Osborn, T. R., "The Design and Performance of Free-Fall Microstructure Instruments at the Institute of Oceanography," University of British Columbia, 10UBC Ms. Rept. 30, 1977, pp. 1-31.
- ⁶Schedvin, J. C., "Microscale Temperature Measurements in the Upper Ocean from a Towed Body," Ph.D. Dissertation, University of California at San Diego, 1979, pp. 1-422.
- ⁷Gibson, C. H., "Fossil Temperature, Salinity and Vorticity Turbulence in the Ocean," *Marine Turbulence*, edited by C. J. Nihoul, Elsevier Press, 1980, pp. 221-257.
- ⁸Osborn, T. R. and Cox, C. S., "Oceanic Fine-Structure," *Geophysical Fluid Dynamics*, Vol. 3, 1972, pp. 321-345.
- ⁹Tennekes, H. and Lumley, J. L., *A First Course in Turbulence*, MIT Press, 1972, pp. 63, 65.
- ¹⁰Wyngaard, J. C. and Coté, O. R., "The Budgets of Turbulent Kinetic Energy and Temperature Variance in the Atmospheric Surface Layer," *Journal of Atmospheric Science*, Vol. 28, March 1971, pp. 190-201.
- ¹¹Osborn, T. R., "Estimates of the Local Rate of Vertical Diffusion from Dissipation Measurements," *Journal of Physical Oceanography*, Vol. 10, Jan. 1980, pp. 83-89.
- ¹²Osborn, T. R. and Bilodeau, L. E., "Temperature Microstructure in the Equatorial Atlantic," *Journal of Physical Oceanography*, Vol. 10, Jan. 1980, pp. 66-82.
- ¹³Gregg, M. C., "Temperature and Salinity Microstructure in the Pacific Equatorial Undercurrent," *Journal of Geophysical Research*, Vol. 81, Feb. 1976, pp. 1180-1196.
- ¹⁴Gregg, M. C., "Variations in the Intensity of Small-Scale Mixing in the Main Thermocline," *Journal of Physical Oceanography*, Vol. 7, May 1977, pp. 436-454.
- ¹⁵Sverdrup, H. U., Johnson, M. W., and Fleming, R. H., *The Oceans*, Prentice Hall, New Jersey, 1942, p. 483.
- ¹⁶Williams, R. B. and Gibson, C. H., "Direct Measurements of Turbulence in the Pacific Equatorial Undercurrent," *Journal of Physical Oceanography*, Vol. 4, Jan. 1974, pp. 104-108.
- ¹⁷von Arx, W. S., *An Introduction to Physical Oceanography*, Addison-Wesley, Reading, Mass., 1974, p. 176.
- ¹⁸Belyaev, V. S., Lubimtzev, M. M., and Ozmidov, R. V., "The Rate of Dissipation of Turbulent Energy in the Upper Layer of the Ocean," *Journal of Physical Oceanography*, Vol. 5, July 1975, pp. 499-505.
- ¹⁹Belyaev, V. S., Gezentsvey, A. N., Monin, A. S., Ozmidov, R. V., and Paka, V. T., "Spectral Characteristics of Small-Scale Fluctuations of Hydrophysical Fields of the Upper Layer of the Ocean," *Journal of Physical Oceanography*, Vol. 5, July 1975, pp. 492-498.
- ²⁰Kolmogoroff, A. N., "A Refinement of Previous Hypotheses Concerning the Local Structure of Turbulence in a Viscous Incompressible Fluid at High Reynolds Number," *Journal of Fluid Mechanics*, Vol. 13, May 1962, pp. 82-85.
- ²¹Gibson, C. H., McConnell, S. O., and Stegen, G. R., "Measurements of the Universal Constant in Kolmogoroff's Third Hypothesis for High Reynolds Number Turbulence," *Physics of Fluids*, Vol. 13, Oct. 1976, pp. 2448-2451.
- ²²Gargett, A. E., Sanford, T. B., and Osborn, T. R., "Surface Mixing Layers in the Sargasso Sea," *Journal of Physical Oceanography*, Vol. 9, Nov. 1979, pp. 1090-1111.
- ²³Gibson, C. H., "Alternative Interpretations for Microstructure Patches in the Thermocline," *Journal of Physical Oceanography*, 1981, submitted.
- ²⁴Gregg, M. C., "Microstructure Patches in the Thermocline," *Journal of Physical Oceanography*, Vol. 10, June 1980, pp. 915-943.
- ²⁵Washburn, L. and Gibson, C. H., "Measurements of Oceanic Microstructure using a Small Conductivity Sensor," *Journal of Geophysical Research*, submitted.
- ²⁶Caldwell, D. R., Dillon, T. M., Brubaker, J. M., Newberger, P. A., and Paulson, C. A., "The Scaling of Vertical Temperature Spectra," *Journal of Geophysical Research*, Vol. 85, April 1980, pp. 1917-1924.
- ²⁷Dillon, T. M. and Caldwell, D. R., "The Batchelor Spectrum and Dissipation in the Upper Ocean," *Journal of Geophysical Research*, Vol. 85, April 1980, pp. 1910-1916.
- ²⁸Gibson, C. H., "Fossil Turbulence and Internal Waves," *American Institute of Physics Proceedings, La Jolla Workshop on Nonlinear Properties of Internal Waves*, University of California at San Diego, La Jolla, Calif., Jan. 15-17, 1980, to be published, 1981.
- ²⁹Stillinger, D. C., and Helland, K. N., UCSD, personal communication. See also Stillinger, D. C., "An Experimental Study of the Transition of Grid Turbulence to Internal Waves in a Salt-Stratified Water Channel," Ph.D. Dissertation, Univ. of California at San Diego, 1981.
- ³⁰Knauss, J. A., "Measurements of the Cromwell Current," *Deep Sea Research*, Vol. 6, No. 4, April 1960, pp. 265-286.
- ³¹Ozmidov, R. V., personal communication, 1979.